Supporting Information

Why are some Enzymes Dimers? Flexibility and Catalysis in *Thermotoga Maritima* Dihydrofolate Reductase

J. Javier Ruiz-Pernía,[†] Iñaki Tuñón,[*†] Vicent Moliner,[*‡] Rudolf K. Allemann[*§]

[†] Departamento de Química Física, Universitat de Valencia, 46100 Burjassot, Valencia, Spain

[‡] Departamento de Química Física y Analítica, Universitat Jaume I, 12071 Castellón, Spain

[§] School of Chemistry, Cardiff University, Main Building, Park Place, Cardiff, CF10 3AT, United Kingdom

[*]corresponding authors:

I. Tuñón: ignacio.tunon@uv.es

V. Moliner: moliner@uji.es

R. K. Allemann: AllemannRK@cardiff.ac.uk

The Supporting Information includes:

Methodological Details

Ensemble Averaged Variational Transition State Theory. As mentioned in the text deviations from classical Transition State Theory (TST) as a result of quantum tunneling effects can be estimated by means of Ensemble-Averaged Variational Transition State Theory (EA-VTST).[1-3] In this approach, the theoretical estimation of the rate constant can be written as in equation (1) of the text.

$$k_{theor}(T) = \Gamma(T,\xi)\frac{k_B T}{h} e^{-\left(\frac{\Delta G_{act}^{QC}(T,\xi)}{RT}\right)} \quad \text{(S1)}$$

ΔG_{act}^{QC} is the quasiclassical activation free energy at the transition state, obtained from the classical mechanical (CM) PMF. It includes a correction for quantizing the vibrations orthogonal to the reaction coordinate and the vibrational free energy of the reactant mode that correlates with motion along the reaction coordinate, calculated as:

$$\Delta G_{act}^{QC} = [W^{CM}(T,\xi^*) + \Delta W_{vib}(T,\xi^*)] - [W^{CM}(T,\xi_R) + \Delta W_{vib,R}(T) + G_{R,T,F}^{CM}] \quad \text{(S2)}$$

where $\Delta W_{vib}(T,\xi^*)$ corrects $W^{CM}(T,\xi^*)$ to account for quantized vibrations orthogonal to the reaction coordinate along which the PMF is defined, ξ, at the maximum of the PMF, ξ^*; $\Delta W_{vib,R}(T)$ corrects $W^{CM}(T,\xi_R)$ for quantized vibrations at the reactant side minimum of the PMF, ξ_R, and is a correction for the vibrational free energy of the reactant mode that correlates with motion along the reaction coordinate.[1]

To correct the classical mechanical PMF, W^{CM}, normal mode analyses were performed for the quantum region atoms. To perform these calculations, in addition to the PMFs obtained as described above, we localized 10 TS structures starting from different configurations of the corresponding simulation windows in the heavy and light enzymes. After tracing the minimum energy path, we optimized 10 reactant structures and obtained the Hessian matrix for all the stationary structures. The final quantum mechanical corrections to the quasi-classical activation free energy at the simulated temperatures (Table S3) were obtained as an average over these structures.

Calculation of the tunneling transmission coefficient. The tunneling transmission coefficients, *κ(T)*, were calculated with the small-curvature tunneling (SCT) approximation, which includes reaction-path curvature appropriate for enzymatic hydride transfers and, in particular, for DHFR.[4-6] The final tunneling contribution (see main text) is obtained as the average over the reaction paths of 10 TS structures.

Calculation of the recrossing transmission coefficient. Grote-Hynes (GH) theory can be applied to describe the evolution of the system along the reaction coordinate at the TS. In particular, the recrossing transmission coefficient, γ(T,ξ), can be obtained as the ratio between the reactive frequency and the equilibrium barrier frequency[7]:

$$\gamma_{GH} = \frac{\omega_r}{\omega_{eq}} \tag{S3}$$

with the equilibrium frequency derived from a parabolic fit of the PMF around the maximum and the reactive frequency ω_r is obtained via the GH equation[8-9]:

$$\omega_r^2 - \omega_{eq}^2 + \omega_r \int_0^\infty \zeta_{TS}(t) e^{-\omega_r t} dt = 0 \tag{S4}$$

$\zeta_{TS}(t)$ is the friction kernel obtained at the TS, assuming that recrossings take place in the proximity of this dynamic bottleneck[9-10]:

$$\zeta(t) = \frac{\langle F_{RC}(0) F_{RC}(t) \rangle}{\mu_{RC} k_B T} \tag{S5}$$

where $F_{RC}(t)$ is the force on the reaction coordinate and μ_{RC} the associated reduced mass. For the evaluation of the TS friction kernel, we ran 50 ps of constrained MD simulations at the top of the PMF. The simulations were carried out at 273, 278, 283, 288, 293, 298, 303, 308, 313, 318, 328 and 338 K. A small time step of 0.05 fs was used to ensure the convergence of the algorithm and forces acting on the reaction coordinate were saved at each simulation step. GH theory has been demonstrated to provide transmission coefficient in very good agreement with those obtained from activated trajectories initiated at the TS ensemble for the methyl transfer reaction catalyzed by cathechol O-methyltransferase[11] and for the hydride transfer

step of formate dehydrogenase.[12] In the case of EcDHFR (Table S1) estimations obtained using the GH equation provides transmission coefficients also close to that previously reported based in trajectory analysis.[13] Thus, the recrossing transmission coefficients, γ, were calculated using eq. S3 for the light and heavy versions of the TmDHFR enzyme prepared as described below. The values obtained at the different temperatures are presented in Table S2. The transmission coefficients of the two versions were found to be statistically different.

Table S1: Transmission coefficients of light and heavy version of EcDHFR evaluated by means of rare events Molecular Dynamics simulations (data from ref 13) and using GH theory at 300 K.

Enzyme	γ_{MD}	γ_{GH}
Light EcDHFR	0.57 ± 0.02	0.59 ± 0.02
Heavy EcDHFR	0.49 ± 0.02	0.52 ± 0.02

Table S2: Transmission coefficients of light and heavy TmDHFR evaluated using GH theory.

Temperature (K)	*Light*	*Heavy*
278	0.61 ± 0.02	0.59 ± 0.01
283	0.61 ± 0.01	0.60 ± 0.02
288	0.60 ± 0.01	0.60 ± 0.01
293	0.61 ± 0.01	0.61 ± 0.02
298	0.61 ± 0.02	0.60 ± 0.01
303	0.60 ± 0.01	0.59 ± 0.01
308	0.59 ± 0.01	0.59 ± 0.02
313	0.60 ± 0.02	0.59 ± 0.01
318	0.59 ± 0.02	0.58 ± 0.01
328	0.58 ± 0.02	0.57 ± 0.02
338	0.57 ± 0.02	0.56 ± 0.02

Table S3. Temperature dependence of the contributions to the rate constant due to: recrossing (γ) tunneling (κ), classical free energy barrier ($\Delta \mathbf{G}_{\mathbf{act}}^{\mathbf{CM}}(\mathbf{T},\boldsymbol{\xi})$), vibrational corrections ($\Delta \mathbf{G}_{\mathbf{vib}}^{\mathbf{QM}}(\mathbf{T})$), vibrational free energy corresponding to the reaction coordinate at the reactants ($\Delta \mathbf{G}_{\boldsymbol{RTF}}^{\boldsymbol{CM}}$), quasi-classical free energy of activation ($\Delta \mathbf{G}_{\boldsymbol{act}}^{\boldsymbol{QC}}$) and effective phenomenological free energies of activation ($\Delta \mathbf{G}_{\boldsymbol{eff}}^{\ddagger}$) as determined from QM/MM calculations. The value derived from the experimental rate constants[14] are also provided ($\Delta \mathbf{G}_{\boldsymbol{exp}}^{\ddagger}$). All free energies are given in kcal·mol^{-1}.

	γ	κ	$\Delta G_{vib}^{QM}(T)$	$\Delta G_{act}^{CM}(T,\xi)$	ΔG_{act}^{QC}	ΔG_{RTF}^{CM}	$\Delta G_{eff}^{\ddagger}$	$\Delta G_{exp}^{\ddagger}$
T = 278 K								
Light	0.61±0.02	5.5±0.8	-2.29±0.04	17.9±0.7	16.02±0.8	0.411±0.011	15.4±1.6	17.89±1.0
Heavy	0.59±0.01	5.1±0.8	-2.23±0.04		16.05±0.7	0.374±0.005	15.4±1.6	17.89±1.0
T = 283 K								
Light	0.61±0.01	5.2±0.7	-2.28±0.04	17.9	16.03±0.8	0.408±0.01	15.4±1.5	18.13±0.9
Heavy	0.60±0.02	4.9±0.7	-2.22±0.04		16.05±0.7	0.371±0.005	15.4±1.5	18.12±0.9
T = 288 K								
Light	0.60±0.01	5.0±0.7	-2.27±0.04	18.0	16.14±0.8	0.405±0.011	15.5±1.5	18.25±0.9
Heavy	0.60±0.01	4.6±0.7	-2.21±0.04		16.16±0.7	0.368±0.005	15.6±1.5	18.25±0.9
T = 293 K								
Light	0.61±0.01	4.7±0.6	-2.26±0.04	18.0	16.14±0.8	0.402±0.011	15.5±1.4	18.35±0.9
Heavy	0.61±0.01	4.4±0.7	-2.20±0.04		16.17±0.7	0.364±0.005	15.6±1.5	18.35±0.9
T = 298 K								
Light	0.61±0.02	4.5±0.6	-2.25±0.04	18.1±0.6	16.25±0.7	0.399±0.011	15.7±1.4	18.44±0.8
Heavy	0.60±0.01	4.2±0.6	-2.19±0.04		16.27±0.6	0.360±0.005	15.7±1.4	18.45±0.8
T = 303 K								
Light	0.59±0.01	4.3±0.5	-2.24±0.04	18.1	16.26±0.7	0.396±0.011	15.7±1.3	18.55±0.8
Heavy	0.59±0.01	4.1±0.6	-2.18±0.04		16.28±0.6	0.356±0.005	15.8±1.4	18.55±0.8
T = 308 K								
Light	0.59±0.01	4.1±0.5	-2.23±0.04	18.3	16.47±0.7	0.392±0.011	15.9±1.3	18.65±0.7
Heavy	0.59±0.02	4.0±0.5	-2.17±0.04		16.49±0.6	0.352±0.005	16.0±1.3	18.66±0.7
T = 313 K								
Light	0.60±0.02	4.0±0.5	-2.22±0.04	18.3	16.47±0.7	0.389±0.011	15.9±1.3	18.74±0.6
Heavy	0.59±0.01	3.9±0.5	-2.16±0.04		16.49±0.6	0.348±0.005	16.0±1.3	18.74±0.6
T = 318 K								
Light	0.59±0.02	3.8±0.4	-2.21±0.04	18.5±0.6	16.68±0.65	0.385±0.010	16.2±1.2	18.85±0.5
Heavy	0.58±0.01	3.7±0.5	-2.15±0.04		16.70±0.64	0.343±0.005	16.2±1.3	18.85±0.5
T = 328 K								
Light	0.58±0.02	3.5±0.5	-2.19±0.04	18.6	16.79±0.65	0.377±0.010	16.3±1.3	19.09±0.3
Heavy	0.58±0.02	3.4±0.4	-2.13±0.04		16.81±0.64	0.334±0.005	16.4±1.2	19.09±0.3
T = 338 K								
Light	0.57±0.02	3.5±0.5	-2.17±0.04	18.7±0.4	16.90±0.55	0.368±0.010	16.4±1.3	19.35±0.1
Heavy	0.56±0.02	3.4±0.4	-2.11±0.04		16.92±0.54	0.324±0.005	16.5±1.2	19.36±0.1

Table S4. Temperature dependence of the contributions for the monomeric version TmDHFR to the rate constant due to: recrossing (γ) tunneling (κ), classical free energy barrier ($\Delta \mathbf{G}_{\mathbf{act}}^{\mathbf{CM}}(\mathbf{T},\boldsymbol{\xi})$), vibrational corrections ($\Delta \mathbf{G}_{\mathbf{vib}}^{\mathbf{QM}}(\mathbf{T})$), vibrational free energy corresponding to the reaction coordinate at the reactants ($\Delta \mathbf{G}_{\boldsymbol{RTF}}^{\boldsymbol{CM}}$), quasi-classical free energy of activation ($\Delta \mathbf{G}_{\boldsymbol{act}}^{\boldsymbol{QC}}$) and effective phenomenological free energies of activation ($\Delta \mathbf{G}_{\boldsymbol{eff}}^{\ddagger}$) as determined from QM/MM calculations. The value derived from the experimental rate constants[14] are also provided ($\Delta \mathbf{G}_{\boldsymbol{exp}}^{\ddagger}$). All free energies are given in kcal·mol^{-1}.

	γ	κ	$\Delta G_{vib}^{QM}(T)$	$\Delta G_{act}^{CM}(T,\xi)$	ΔG_{act}^{QC}	ΔG_{RTF}^{CM}	$\Delta G_{eff}^{\ddagger}$
T = 278 K							
Light	0.66±0.01	5.0±0.8	-1.80±0.04	17.6±0.5	16.23±0.64	0.435±0.010	15.57±1.2
Heavy	0.66±0.01	4.9±0.8	-1.80±0.04		16.21±0.61	0.415±0.006	15.56±1.2
T = 298 K							
Light	0.55±0.01	4.2±0.7	-1.77±0.04	18.3±0.7	16.96±0.74	0.426±0.010	16.46±1.6
Heavy	0.54±0.01	4.1±0.6	-1.77±0.04		16.93±0.73	0.405±0.005	16.46±1.6
T = 318 K							
Light	0.44±0.02	3.6±0.4	-1.74±0.04	19.2±1.0	17.87±1.04	0.414±0.010	17.57±1.9
Heavy	0.41±0.01	3.5±0.5	-1.74±0.04		17.85±1.03	0.391±0.005	17.60±1.9

Table S5. Averaged structural parameters of the reactant state, RS, and transition state, TS, from the PMFs of TmDHFR obtained at 278, 298, 318 and 338 K. Distances are in Å and angles in degrees.

	278		338	
	RS	**TS**	**RS**	**TS**
$(C4_{cofac}\text{-}H_t)\text{-}d(C6_{subs}\text{-}H_t)$	-2.07	-0.24	-2.07	-0.25
$d(C4_{cofac}\text{-}C6_{subs})$	4.23±0.1	2.64±0.1	4.23±0.1	2.62±0.1
$d(C4_{cofac}\text{-}H_t)$	1.10±0.03	1.22±0.03	1.10±0.03	1.22±0.03
$d(C6_{subs}\text{-}H_t)$	3.17±0.04	1.47±0.04	3.18±0.04	1.47±0.04
$d(HN7_{cof}\text{-}O_{ILE15})$	2.6±0.5	3.3±0.7	2.8±0.5	3.1±0.6
$d(HN7_{cof}\text{-}O_{ALA8})$	2.3±0.3	2.0±0.2	2.2±0.3	2.0±0.2
$d(O7_{cof}\text{-}HN_{ALA8})$	4.6±0.4	4.6±0.2	4.1±0.3	4.7±0.2
$d(N8_{subs}\text{-}N^{\varepsilon}{}_{ARG28})$	3.8±0.3	3.1±0.1	3.9±0.3	2.8±0.1
$d(N8_{subs}\text{-}N^{\eta 1}{}_{ARG28})$	3.6±0.3	3.5±0.1	3.7±0.3	3.6±0.1
$d(N2_{subs}\text{-}O\delta_{ASP27})$	2.7±0.1	2.7±0.1	2.9±0.2	2.7±0.1
$d(N2_{subs}\text{-}O\varepsilon_{ASP27})$	3.5±0.2	3.4±0.2	3.0±0.2	4.1±0.2
$d(H5_{subs}\text{-}O_{ILE100})$	2.2±0.2	2.8±0.5	2.0±0.2	3.2±0.7
$(C4_{cofac}\text{–}H_t\text{–}C6_{subs})$	162±8	159±7	161±9	158±8

	298		318	
	RS	**RS**	**RS**	**TS**
$d(C4_{cofac}\text{-}H_t)\text{-}d(C6_{subs}\text{-}H_t)$	-2.07	-0.23	-2.07	-0.23
$d(C4_{cofac}\text{-}C6_{subs})$	4.23±0.1	2.63±0.1	4.21±0.1	2.63±0.1
$d(C4_{cofac}\text{-}H_t)$	1.10±0.03	1.22±0.03	1.10±0.03	1.23±0.03
$d(C6_{subs}\text{-}H_t)$	3.18±0.04	1.46±0.04	3.18±0.04	1.46±0.04
$d(HN7_{cof}\text{-}O_{ILE15})$	2.2±0.3	2.7±0.5	2.8±0.4	3.1±0.6
$d(HN7_{cof}\text{-}O_{ALA8})$	2.5±0.3	2.0±0.2	2.1±0.2	2.0±0.2
$d(O7_{cof}\text{-}HN_{ALA8})$	4.9±0.5	4.6±0.2	4.3±0.3	4.6±0.2
$d(N8_{subs}\text{-}N^{\varepsilon}{}_{ARG28})$	3.9±0.3	3.2±0.2	3.7±0.3	3.0±0.1
$d(N8_{subs}\text{-}N^{\eta 1}{}_{ARG28})$	3.5±0.2	3.5±0.1	3.4±0.2	3.6±0.2
$d(N2_{subs}\text{-}O\delta_{ASP27})$	2.8±0.1	2.8±0.1	2.8±0.1	2.7±0.1
$d(N2_{subs}\text{-}O\varepsilon_{ASP27})$	3.6±0.3	3.5±0.3	3.5±0.3	3.3±0.2
$d(H5_{subs}\text{-}O_{ILE100})$	2.2±0.2	2.6±0.3	2.3±0.3	2.8±0.4
$(C4_{cofac}\text{–}H_t\text{–}C6_{subs})$	161±9	162±7	159±9	160±7

Table S6. Averaged structural parameters of the reactant state, RS, and transition state, TS, from 2 ns QM/MM MD simulations of the windows corresponding to the reactant and transition state of the hydride transfer in EcDHFR at 298. Distances are in Å and angles in degrees. Data from ref 15.[15]

	RS	**TS**
$C4_{cofac}$ –H_t- $C6_{subs}$	141±15	163±7
d ($C4_{cofac}$ –H_t)- d ($C6_{subs}$-H_t)	-1.9±0.4	-0.18±0.04
d ($C4_{cofac}$- $C6_{subs}$)	3.9±0.2	2.63±0.06
d ($C4_{cofac}$ –H_t)	1.09±0.03	1.24±0.03
d ($C6_{subs}$-H_t)	2.9±0.4	1.42±0.04
d ($HN7N_{cofac}$-O_{ALA7})	2.2±0.5	2.1±0.2
d ($HN7N_{cofac}$-N_{ALA7})	3.7±0.5	3.5±0.2
d ($HN7N_{cofac}$ -S_{MET20})	4.6±0.7	2.6±0.3
d ($HO3_{cofac}$-$N\delta_{ASN18}$)	3.8±0.6	4.1±0.6
d ($HO2_{cofac}$-O_{ALA19})	3.2±0.4	3.2±0.5
d ($HO2_{cofac}$-N_{ALA19})	3.1±0.2	3.0±0.2
d ($HN7N_{cofac}$-O_{ILE14})	3.0±0.9	3.5±0.4
d ($HN5_{subs}$ -S_{MET20})	3.1±0.4	2.9±0.4
d ($HN3_{subs}$-$O\delta_{ASP27}$)	1.8±0.1	1.9±0.2
d ($HN2_{subs}$-$O\delta_{ASP27}$)	1.8±0.2	1.8±0.1

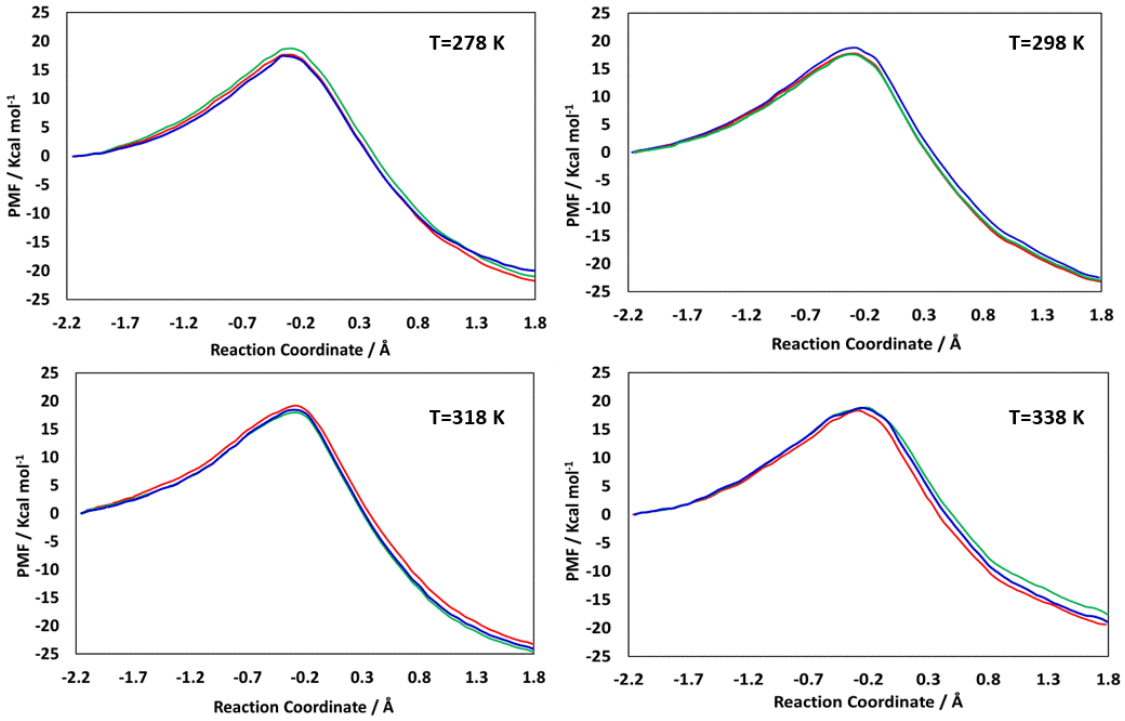

Figure S1. AM1-SRP/MM PMFs, $\Delta G_{act}^{CM}(T,\xi)$, obtained at four different temperatures starting from different TS configurations. The reaction coordinate is the antisymmetric combination of distances describing the hydride transfer.

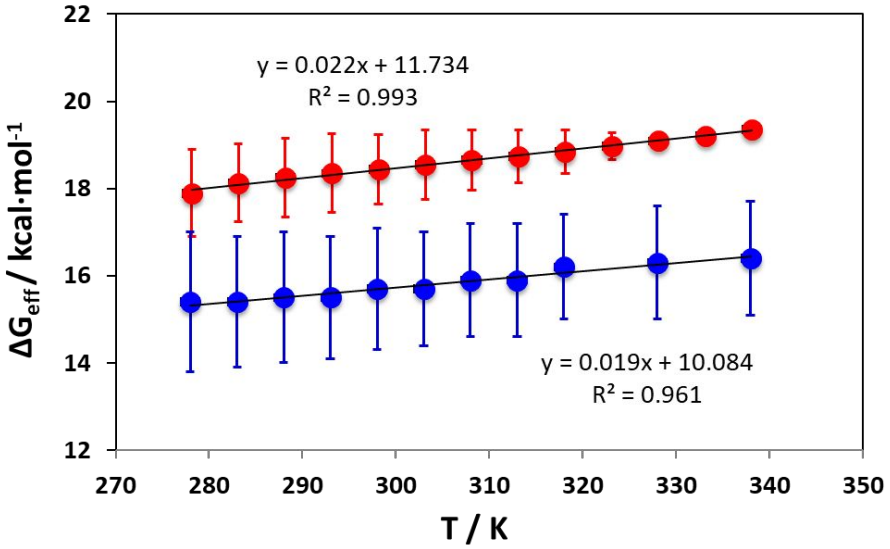

Figure S2. Experimental (red) and theoretical (blue) effective activation free energies versus temperature for the dimeric TmDHFR. Error bars are indicated as vertical lines.

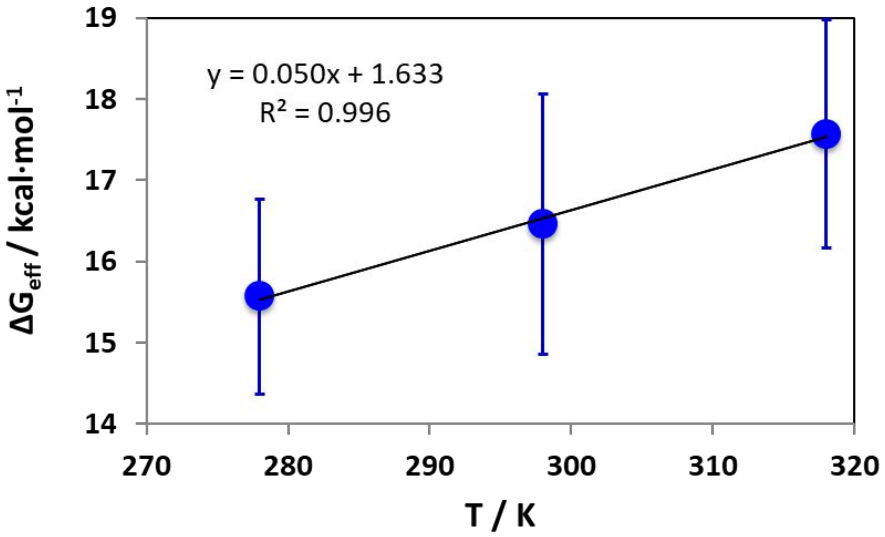

Figure S3. Calculated effective activation free energies versus temperature for the monomeric TmDHFR.

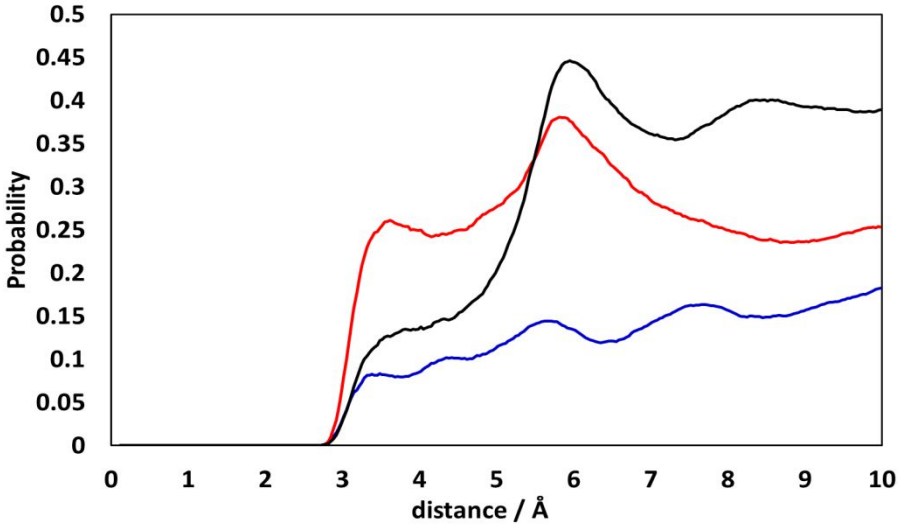

Figure S4. Radial Distribution Function around N5 for EcDHFR (blue line), TmDHFR dimer (black line) and TmDHFR monomer (red line).

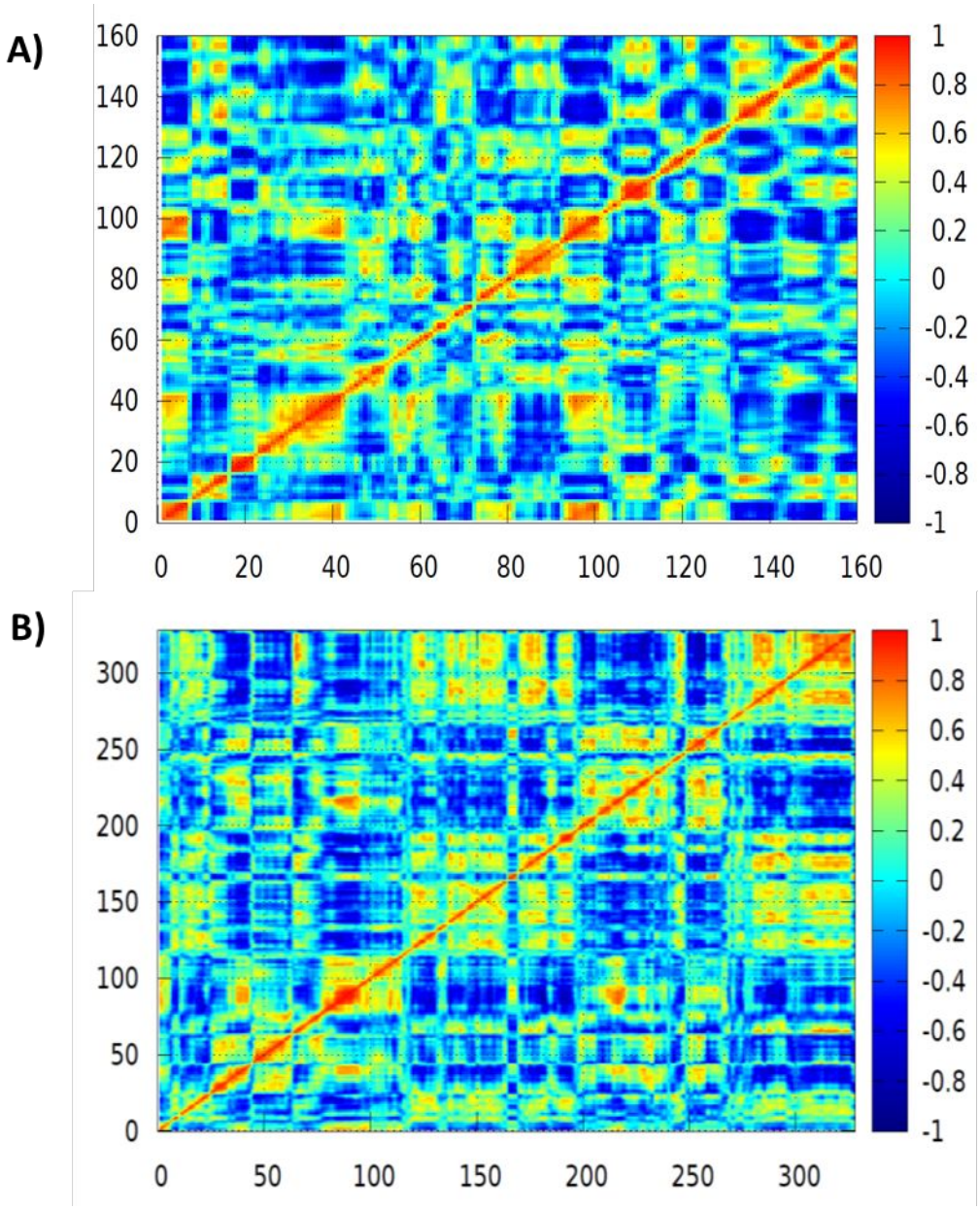

Figure S5. Cross-correlation matrixes obtained from 50 ns MD simulations at 298 K for: a) the monomer of TmDHFR, b) the full dimer of TmDHFR.

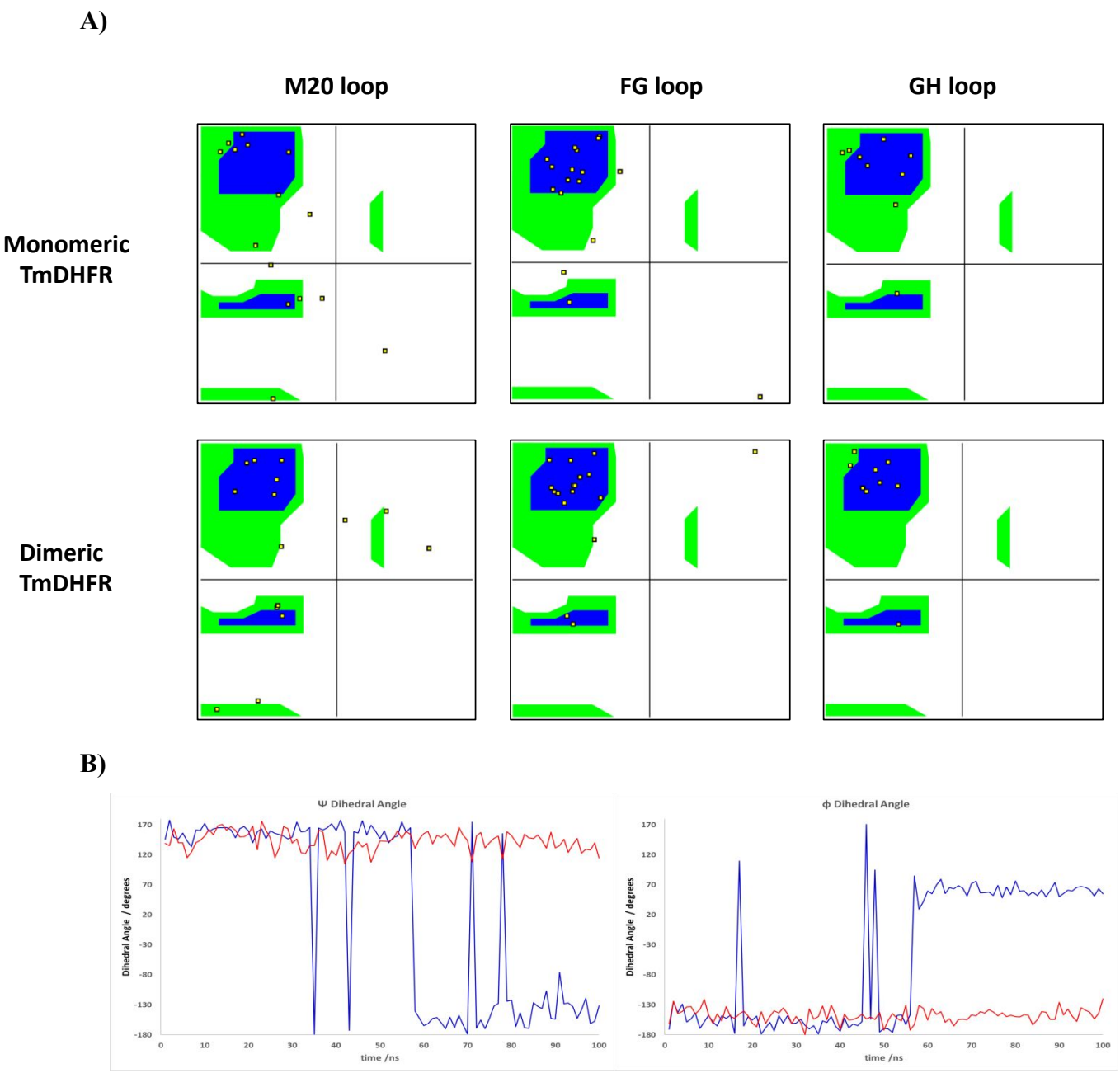

Figure S6. A) Ramachandran plots for the M20, FG and GH loops of monomeric and dimeric TmDHFR obtained after 50 ns MD simulations. The yellow points represent the pair of φ and ψ values for each residue of the loops. Significant differences are observed only for the M20 loop. B) Time evolution of the φ and ψ dihedral angles of residue 16 in the monomeric (blue) and dimeric form (red) of TmDHFR.

References

1. Alhambra, C.; Corchado, J.; Sánchez, M. L.; Garcia-Viloca, M.; Gao, J.; Truhlar, D. G., Canonical Variational Theory for Enzyme Kinetics with the Protein Mean Force and Multidimensional Quantum Mechanical Tunneling Dynamics. Theory and Application to Liver Alcohol Dehydrogenase, *J. Phys. Chem. B* **2001,** 105, 11326-11340.
2. Truhlar, D. G.; Gao, J. L.; Alhambra, C.; Garcia-Viloca, M.; Corchado, J.; Sanchez, M. L.; Villa, J., The Incorporation of Quantum Effects in Enzyme Kinetics Modeling, *Acc. Chem. Res.* **2002,** 35, 341-349.
3. Truhlar, D. G.; Gao, J.; Garcia-Viloca, M.; Alhambra, C.; Corchado, J.; Luz Sanchez, M.; Poulsen, T. D., Ensemble-Averaged Variational Transition State Theory with Optimized Multidimensional Tunneling for Enzyme Kinetics and other Condensed-Phase Reactions, *Int. J. Quant. Chem.* **2004,** 100, 1136-1152.
4. Pu, J.; Gao, J.; Truhlar, D. G., Multidimensional Tunneling, Recrossing, and the Transmission Coefficient for Enzymatic Reactions, *Chem. Rev.* **2006,** 106, 3140-3169.
5. Pang, J.; Pu, J.; Gao, J.; Truhlar, D. G.; Allemann, R. K., Hydride Transfer Reaction Catalyzed by Hyperthermophilic Dihydrofolate Reductase Is Dominated by Quantum Mechanical Tunneling and Is Promoted by Both Inter- and Intramonomeric Correlated Motions, *J. Am. Chem. Soc.* **2006,** 128, 8015-8023.
6. Garcia-Viloca, M.; Truhlar, D. G.; Gao, J., Reaction-Path Energetics and Kinetics of the Hydride Transfer Reaction Catalyzed by Dihydrofolate Reductase, *Biochemistry* **2003,** 42, 13558-13575.
7. Gertner, B. J.; Wilson, K. R.; Hynes, J. T., *Nonequilibrium Solvation Effects on Reaction Rates for Model S_N2 Reactions in Water*, *J. Chem. Phys.* **1989,** 90, 3537-3558.
8. Grote, R. F.; Hynes, J. T., The Stable States Picture of Chemical Reactions. II. Rate Constants for Condensed and Gas Phase Reaction Models, *J. Chem. Phys.* **1980,** 73, 2715-2732.
9. Hynes, J. T.; Baer, M., The Theory of Chemical Reaction Dynamics. Boca Raton: Florida, **1985**.
10. Kim, H. J.; Hynes, J. T., A Theoretical Model for S_N1 Ionic Dissociation in Solution. I. Activation Free Energetics and Transition-State Structure, *J. Am. Chem. Soc.* **1992,** 114, 10508-10528.
11. Roca, M.; Moliner, V.; Tunon, I.; Hynes, J. T., Coupling Between Protein and Reaction Dynamics in Enzymatic Processes: Application of Grote-Hynes Theory to Catechol O-Methyltransferase, *J.Am. Chem. Soc.* **2006,** 128, 6186-6193.
12. Roca, M.; Oliva, M.; Castillo, R.; Moliner, V.; Tuñón, I., Do Dynamic Effects Play a Significant Role in Enzymatic Catalysis? A Theoretical Analysis of Formate Dehydrogenase, *Chemistry Eur. J.* **2010,** 16, 11399-11411.
13. Luk, L. Y. P.; Ruiz-Pernia, J. J.; Dawson, W. M.; Roca, M.; Loveridge, E. J.; Glowacki, D. R.; Harvey, J. N.; Mulholland, A. J.; Tuñón, I.; Moliner, V.; Allemann, R. K., Unraveling the Role of Protein Dynamics in Dihydrofolate Reductase Catalysis, *Proc. Natl. Acad. Sci. USA* **2013,** 110, 16344-16349.
14. Luk, L. Y.; Loveridge, E. J.; Allemann, R. K., Different Dynamical Effects in Mesophilic and Hyperthermophilic Dihydrofolate Reductases, *J. Am. Chem. Soc.* **2014,** 136, 6862-6865.
15. Ruiz-Pernía, J. J.; Luk, L. Y.; García-Meseguer, R.; Martí, S.; Loveridge, E. J.; Tuñón, I.; Moliner, V.; Allemann, R. K., Increased Dynamic Dffects in a Catalytically Compromised Variant of Escherichia Coli Dihydrofolate Reductase, *J. Am. Chem. Soc.* **2013,** 135, 18689-18696.